Available online at www.sciencedirect.com
ScienceDirect
Journal of Computational Physics 227 (2007) 36–54
JOURNAL OF COMPUTATIONAL PHYSICS
www.elsevier.com/locate/jcp

Spectral solvers for spherical elliptic problems

F. Auteri *, L. Quartapelle

Dipartimento di Ingegneria Aerospaziale, Politecnico di Milano, Via La Masa 34, 20156 Milano, Italy

Received 10 November 2006; received in revised form 6 July 2007; accepted 9 July 2007
Available online 31 July 2007

Abstract

A new family of direct spectral solvers for the 3D Helmholtz equation in a spherical gap and inside a sphere for non-axisymmetric problems is presented. A variational formulation (no collocation) is adopted, based on the Fourier expansion and the associated Legendre functions to represent the angular dependence over the sphere and using basis functions generated by Legendre or Jacobi polynomials to represent the radial structure of the solution. In the present method, boundary conditions on the polar axis and at the sphere center are not required and never mentioned, by construction. The spectral solution of the vector Dirichlet problem is also considered, by employing a transformation that uncouples the spherical components of the Fourier modes and that is implemented here for the first time. The condition numbers of the matrices involved in the scalar solvers are computed and the spectral convergence of all the proposed solution algorithms is verified by numerical tests.

1. Introduction

Several widely studied problems of computational physics can be naturally set as vector elliptic problems in a three-dimensional spherical coordinate system. Of particular interest is the case of Helmholtz vector problems, since they arise, for instance, in the time advancement of Navier–Stokes equations by fractional step methods. Problems of mathematical physics can be set both in an open domain extending to infinity or in closed domains. In this work we are particularly concerned with problems in closed domains.

When considering vector fields described by the components which more naturally fit the spherical symmetry of the domain, namely radial, azimuthal and zenithal, a coupling between equations for the different components arises. Such coupling compromises the possibility to separate variables in the solution process. Two strategies have been devised, in the past, to tackle this problem. The most obvious one, quite rude though, is to convert the vector field to Cartesian components, then solve the decoupled elliptic problem and return to spherical components. Otherwise, one can employ vector spherical harmonics, see for instance [16,17]. A third technique was proposed by the second author [13], and applies to the equations of motion already discretised in the longitude dimension.

* Corresponding author. Tel.: +39 02 2399 8393; fax: +39 02 2399 8334.
E-mail address: auteri@aero.polimi.it (F. Auteri).

0021-9991/$ - see front matter © 2007 Elsevier Inc. All rights reserved.
doi:10.1016/j.jcp.2007.07.011

Once the problem is uncoupled and reduced to the solution of scalar Helmholtz equations, several different combinations of spectral and finite difference methods have been proposed for it so far. For instance in [6] a 2D Fourier spectral representation is combined with finite differences in the radial direction. The first fully spectral numerical approach employing associated Legendre functions for the longitude and latitude and Legendre polynomials for the radial direction was proposed in [10]. Chebyshev polynomials have also been employed, see for instance [7,11,8]. Moreover, the use of first and second kind Chebyshev polynomials for even and odd Fourier modes, respectively, has been advocated to overcome the difficulties at the center in [4]. By contrast, the use of only even order Chebyshev polynomials is considered in [9] to overcome the same difficulty. A detailed discussion of the cylindrical and spherical coordinate singularities and of their treatment in collocation spectral methods is given by Boyd [5].

In this paper a fully spectral solver for the 3D, non axisymmetric, vector Helmholtz–Dirichlet problem is proposed. The vector Helmholtz problem is decomposed to scalar Helmholtz problems by resorting to the technique proposed by the second author in [13]. The method is based on scalar spherical harmonics in the two angular coordinates and features two distinct polynomial bases in the radial direction, one employing the Legendre basis proposed by Shen [15] for the spherical gap, the other developed here originally for the problem including the sphere centre. For completeness, we also include a scalar solver for the Helmholtz–Neumann problem both for the spherical gap and for the full sphere exploiting, in the radial direction, normalised Legendre polynomials and the new polynomial basis, respectively.

A distinct advantage of the spectral methods here proposed exploiting spherical harmonics, with respect to Fourier methods [12,15], is that they do not suffer from the renowned pole problem. Moreover, the spectral basis proposed for the radial direction for the problem in the full sphere also satisfies all the regularity conditions in the sphere centre, so that no "centre problem" arises as well.

2. Scalar Helmholtz equation in spherical coordinates

Let us consider the Helmholtz equation in spherical coordinates, with unknown $u = u(r,\theta,\phi)$:

$$(-\nabla^2 + \gamma)u = f(r,\theta,\phi), \tag{2.1}$$

where γ is a non-negative constant, $f(r,\theta,\phi)$ is a known source term defined inside a spherical gap or a sphere and ∇^2 is the Laplace operator in spherical coordinates

$$\nabla^2 \equiv \frac{1}{r^2}\frac{\partial}{\partial r}\left(r^2\frac{\partial}{\partial r}\right) + \frac{1}{r^2\sin\theta}\frac{\partial}{\partial\theta}\left(\sin\theta\frac{\partial}{\partial\theta}\right) + \frac{1}{r^2\sin^2\theta}\frac{\partial^2}{\partial\phi^2}. \tag{2.2}$$

Since the datum $f(r,\theta,\phi)$ is real and periodic in ϕ, it can be expanded by means of a real Fourier series, namely,

$$f(r,\theta,\phi) = f_0(r,\theta) + 2\sum_{m=1}^{\infty}[f_m(r,\theta)\cos(m\phi) - f_{-m}(r,\theta)\sin(m\phi)], \tag{2.3}$$

where the expansion coefficients $f_m(r,\theta)$, $m = 0, \pm 1, \pm 2, \ldots$, are defined by

$$f_{\pm m}(r,\theta) = \frac{1}{2\pi}\int_0^{2\pi} f(r,\theta,\phi)\quad \begin{matrix}\cos(m\phi)\\ \sin(m\phi)\end{matrix}\, \mathrm{d}\phi. \tag{2.4}$$

The real unknown u is expanded in the same Fourier series.

Introducing these expansions in the differential Eq. (2.1), equating similar terms and simplifying, we obtain an infinite system of uncoupled equations

$$-\frac{1}{r^2}\frac{\partial}{\partial r}\left(r^2\frac{\partial u_m}{\partial r}\right) - \frac{1}{r^2\sin\theta}\frac{\partial}{\partial\theta}\left(\sin\theta\frac{\partial u_m}{\partial\theta}\right) + \frac{m^2}{r^2\sin^2\theta}u_m + \gamma u_m = f_m(r,\theta), \tag{2.5}$$

for $m = 0, \pm 1, \pm 2, \ldots$. To discretise the problem we start by truncating the series at a suitable integer $M_t > 0$, so that $-M_t + 1 \leqslant m \leqslant M_t$ and the Fourier expansions above are approximated by *finite* summations; for instance, the truncated expansion of the unknown is

$$u(r,\theta,\phi) = u_0(r,\theta) + 2\sum_{m=1}^{M_t-1}[u_m(r,\theta)\cos(m\phi) - u_{-m}(r,\theta)\sin(m\phi)] + u_{M_t}(r,\theta)\cos(M_t\phi), \tag{2.6}$$

where the absence of the coefficient *2* in front of last term must be noticed.

To formulate the considered elliptic problem in variational form, the Eq. (2.5) for the Fourier coefficient is multiplied by $r^2\sin^2\theta$, which yields

$$-\sin^2\theta\frac{\partial}{\partial r}\left(r^2\frac{\partial u_m}{\partial r}\right) - \sin\theta\frac{\partial}{\partial\theta}\left(\sin\theta\frac{\partial u_m}{\partial\theta}\right) + m^2u_m + \gamma r^2\sin^2\theta\ u_m = r^2\sin^2\theta\ f_m(r,\theta), \tag{2.7}$$

for $m = 0, \pm 1, \pm 2, \ldots, \pm(M_t-1), M_t$.

To represent the solution $u_m(r,\theta)$, with $-M_t + 1 \leqslant m \leqslant M_t$, let us introduce the associated Legendre functions $\{P_\ell^m(z), \ell = m, m+1, \ldots, \text{for } m = 0,1,2,\ldots\}$. These functions are solution to the ordinary differential equation

$$\sin\theta\frac{\mathrm{d}}{\mathrm{d}\theta}\left(\sin\theta\frac{\mathrm{d}P_\ell^m(\cos\theta)}{\mathrm{d}\theta}\right) + [\ell(\ell+1)\sin^2\theta - m^2]P_\ell^m(\cos\theta) = 0 \tag{2.8}$$

and satisfy the following orthogonality relation

$$\int_0^\pi P_\ell^m(\cos\theta)P_{\ell'}^m(\cos\theta)\sin\theta\ \mathrm{d}\theta = \frac{2}{2\ell+1}\frac{(\ell+m)!}{(\ell-m)!}\delta_{\ell,\ell'}. \tag{2.9}$$

As well known, this set of functions, once combined with the exponential $\mathrm{e}^{\mathrm{i}m\phi}$, $m = 0,1,2,\ldots$, or, equivalently, the trigonometric functions $\cos(m\phi)$ and $\sin(m\phi)$, provides a complete basis for representing the dependence on the angular coordinates θ and ϕ over the unit sphere.

We will employ the fully orthonormalised version of the associated Legendre functions, defined by

$$\widehat{P}_\ell^m(z) \equiv \sqrt{\frac{2\ell+1}{2}\frac{(\ell-m)!}{(\ell+m)!}}\,P_\ell^m(z). \tag{2.10}$$

The solution $u_m(r,\theta)$, with $-M_t + 1 \leqslant m \leqslant M_t$, is expanded in the series

$$u_m(r,\theta) = \sum_{\ell=|m|}^{M_t} u_\ell^m(r)\widehat{P}_\ell^{|m|}(\cos\theta). \tag{2.11}$$

Substituting the expansion (2.11) into the Eq. (2.7) and exploiting Eq. (2.8) satisfied by the associated Legendre functions $\widehat{P}_\ell^m(\cos\theta)$, we obtain

$$\sum_{\ell=|m|}^{M_t}\left\{-\frac{\mathrm{d}}{\mathrm{d}r}\left(r^2\frac{\mathrm{d}u_\ell^m}{\mathrm{d}r}\right) + [\ell(\ell+1) + \gamma r^2]u_\ell^m\right\}\widehat{P}_\ell^{|m|}(\cos\theta) = r^2 f_m(r,\theta). \tag{2.12}$$

By projecting this equation onto the basis of the associated Legendre functions and exploiting their orthogonality, we obtain the following ordinary differential modal equation

$$-\frac{\mathrm{d}}{\mathrm{d}r}\left(r^2\frac{\mathrm{d}u_\ell^m}{\mathrm{d}r}\right) + [\ell(\ell+1) + \gamma r^2]u_\ell^m = r^2 g_\ell^m(r), \tag{2.13}$$

where

$$g_\ell^m(r) = \int_0^\pi f_m(r,\theta)\widehat{P}_\ell^{|m|}(\cos\theta)\sin\theta\ \mathrm{d}\theta. \tag{2.14}$$

Thus, the solution of the three-dimensional elliptic equation is reduced to a set of uncoupled 1D, second-order ordinary differential equations for the expansion coefficients $u_\ell^m(r)$, for $-M_t + 1 \leqslant m \leqslant M_t$ and $|m| \leqslant \ell \leqslant M_t$. The integral over the angular variable θ is evaluated by means of the Gauss–Legendre quadrature formula for the transformed variable $z = \cos\theta$, using $M_t + 2$ integration points. This gives a *nearly* uniform distribution of values for θ, with the polar extremes excluded.

3. Spherical gap

The Helmholtz equation is first solved in the spherical annular domain $[r_i \leqslant r \leqslant r_o]$, supplemented by either Neumann or Dirichlet boundary condition. In both cases the modal equations are rewritten in dimensionless form by introducing a dimensionless radial coordinate x defined by $r = r(x) = E(\alpha + x)$, with $E \equiv (r_o - r_i)/2$ and $\alpha \equiv (r_i + r_o)/(r_o - r_i)$, such that the interval $[r_i \leqslant r \leqslant r_o]$ is mapped in $[\{-1\} \leqslant x \leqslant 1]$. The modal equation for the transformed unknown $v_\ell^m(x) = u_\ell^m(r)$, which will be still denoted by the same letter u_ℓ^m as $u_\ell^m = u_\ell^m(x)$, will be

$$-\frac{1}{E^2}\frac{\mathrm{d}}{\mathrm{d}x}\left[(\alpha+x)^2\frac{\mathrm{d}u_\ell^m}{\mathrm{d}x}\right] + \left[\frac{\ell(\ell+1)}{E^2} + \gamma(\alpha+x)^2\right]u_\ell^m = (\alpha+x)^2 g_\ell^m(r(x)). \tag{3.1}$$

The weak form of this modal equation for $u_\ell^m(x)$, is obtained by multiplying the equation by suitable functions $v(x)$ and integrating over the interval $[-1,1]$. An integration by parts gives

$$\begin{aligned}&\int_{-1}^{1}\left\{\frac{(\alpha+x)^2}{E^2}\frac{\mathrm{d}v}{\mathrm{d}x}\frac{\mathrm{d}u_\ell^m}{\mathrm{d}x} + \left[\frac{\ell(\ell+1)}{E^2} + \gamma(\alpha+x)^2\right]vu_\ell^m\right\}\mathrm{d}x \\ &\quad = \int_{-1}^{1}(\alpha+x)^2 v(x)\; g_\ell^m(r(x))\;\mathrm{d}x + \frac{1}{E^2}\left[(\alpha+x)^2 v(x)\frac{\mathrm{d}u_\ell^m(x)}{\mathrm{d}x}\right]\Bigg|_{-1}^{1}.\end{aligned} \tag{3.2}$$

3.1. Neumann problem

Let us assume that the Helmholtz equation for u is supplemented by Neumann boundary condition on the two spherical surfaces $r = r_i$ and $r = r_o$, namely,

$$\frac{\partial u}{\partial r}_{|r=r_{i,o}} = b^{i,o}(\theta,\phi), \tag{3.3}$$

where $b^{i,o}(\theta,\phi)$ are the boundary data for $r = r_i$ and $r = r_o$. If $\gamma = 0$, the data of the Neumann problem, i.e., the source term f and the boundary values $b^{i,o}$ should satisfy the compatibility condition $\int_\Omega f = -\int_{\partial\Omega} b$, with Ω is the spherical gap domain, under which the solution is defined up to an additive constant.

The counterpart of the Neumann boundary condition for the transformed unknown $u_\ell^m(x)$ reads

$$\frac{\mathrm{d}u_\ell^m}{\mathrm{d}x}_{|x=\mp 1} = E b_\ell^{m,i,o}, \tag{3.4}$$

where the coefficients $b_\ell^{m,i,o}$ are the transform of the boundary value functions $b^{i,o}(\theta,\phi)$ similar to that given by relation (2.14). Thus, the weak equation incorporating the Neumann boundary condition is Eq. (3.2) with the last term on the right-hand side replaced by $-\left(r_i^2/E^3\right)v(-1)b_\ell^{m,i} + \left(r_o^2/E^3\right)v(1)b_\ell^{m,o}$.

The approximate solution $u_\ell^{\pm m}(x)$ of the Neumann boundary value problem is expanded[1] in the series

$$u_\ell^{\pm m}(x) = \sum_{i=0}^{N}\hat{u}_{\ell;i}^{\pm m}\widehat{L}_i(x), \tag{3.5}$$

where the elements of the basis $\{\widehat{L}_i(x)\}$ are the *normalised* Legendre polynomials, namely, for $i \geqslant 0$, $\widehat{L}_i(x) \equiv \sqrt{i+\frac{1}{2}}\,L_i(x)$. In the following the "hat" will be used to distinguish any quantity defined in terms of the normalised Legendre polynomials. The overall expansion of the unknown $u(r,\theta,\phi)$ to the Neumann problem in a spherical gap is

[1] In the matrix equations of the solution algorithm, the Fourier index m is assumed to be always positive and the presence of the components with negative values of the index is taken into account by appending the label $\pm m$ to the Fourier expansion coefficients.

$$u(r,\theta,\phi)=\sum_{\ell=0}^{M_t}\left[\sum_{i=0}^{N}\hat{u}^0_{\ell;i}\widehat{L}_i\Big(\alpha+\frac{r}{E}\Big)\right]\widehat{P}^0_\ell(\cos\theta)+2\left\{\sum_{\ell=m}^{M_t}\left[\sum_{i=0}^{N}\hat{u}^{\pm m}_{\ell;i}\widehat{L}_i\Big(\alpha+\frac{r}{E}\Big)\right]\widehat{P}^{|m|}_\ell(\cos\theta)\right\}\begin{matrix}\cos(m\phi)\\-\sin(m\phi)\end{matrix}\overset{M_t-1}{\underset{m=1}{\sum}}$$
$$+\left[\sum_{i=0}^{N}\hat{u}^{M_t}_{M_t;i}\widehat{L}_i\Big(\alpha+\frac{r}{E}\Big)\right]\widehat{P}^{M_t}_{M_t}(\cos\theta)\cos(M_t\phi). \tag{3.6}$$

The inverted summation symbol is used to denote the summation over the third, and therefore right-most, index m of the array of the expansion coefficients. Moreover, the presence of superposed cosine and sine functions means that two distinct series are involved by the Fourier summation.

By choosing the weighting functions $v(x)$ in the same approximation space used for the unknown $u^{\pm m}_\ell(x)$, the weak variational formulation of the modal equation yields the following system of linear equations

$$\left[\frac{1}{E^2}\widehat{D}+\frac{\ell(\ell+1)}{E^2}\hat{I}+\gamma\widehat{M}\right]\hat{u}^{\pm m}_\ell=\hat{g}^{\pm m}_\ell+\langle\text{b.t.}\rangle^{\pm m}_\ell. \tag{3.7}$$

In the equation system above,[2] $\hat{I}$ is identity matrix of order $N+1$ while matrices $\widehat{D}$ and $\widehat{M}$, representing the radial operators, are defined by

$$\begin{aligned}\widehat{D}_{i,i'}&=\int_{-1}^{1}(\alpha+x)^2\frac{\mathrm{d}\widehat{L}_i(x)}{\mathrm{d}x}\frac{\mathrm{d}\widehat{L}_{i'}(x)}{\mathrm{d}x}\mathrm{d}x,\\ \widehat{M}_{i,i'}&=\int_{-1}^{1}(\alpha+x)^2\widehat{L}_i(x)\widehat{L}_{i'}(x)\ \mathrm{d}x,\end{aligned} \tag{3.8}$$

for $0\leqslant(i,i')\leqslant N$. Matrix $\widehat{D}$ is full and its elements are evaluated numerically by means of Gauss–Legendre quadrature using $N+1$ integration points. On the contrary, matrix $\widehat{M}$ is penta-diagonal and its elements can be determined in closed form

$$\widehat{M}=\begin{pmatrix}\hat{c}_0&\hat{b}_0&\hat{a}_0&&&&\\ \hat{b}_0&\hat{c}_1&\hat{b}_1&\hat{a}_1&&&\\ \hat{a}_0&\hat{b}_1&\ddots&\ddots&\ddots&&\\ &\hat{a}_1&\ddots&\ddots&\ddots&\hat{a}_{N-2}&\\ &&\ddots&\ddots&\ddots&\hat{b}_{N-1}&\\ &&&\hat{a}_{N-2}&\hat{b}_{N-1}&\hat{c}_N\end{pmatrix} \tag{3.9}$$

where

$$\begin{aligned}\hat{a}_i&=\frac{(i+1)(i+2)}{(2i+3)\sqrt{(2i+1)(2i+5)}},\quad i\geqslant 0,\\ \hat{b}_i&=2\alpha\frac{i+1}{\sqrt{(2i+1)(2i+3)}},\quad \geqslant 0,\\ \hat{c}_i&=\alpha^2+\frac{2i^2+2i-1}{(2i-1)(2i+3)},\quad i\geqslant 0.\end{aligned} \tag{3.10}$$

For the proof, see [3].

As far as the right-hand side is concerned, the components of source vector and of the boundary term are

$$\hat{g}^{\pm m}_{\ell;i}=\int_{-1}^{1}\widehat{L}_i(x)(\alpha+x)^2 g^{\pm m}_\ell(r(x))\ \mathrm{d}x, \tag{3.11}$$

$$\langle\text{b.t.}\rangle^{\pm m}_{\ell;i}=-\frac{r_{\mathrm{i}}^2}{E^3}\widehat{L}_i(-1)\ b^{\pm m,\mathrm{i}}_\ell+\frac{r_{\mathrm{o}}^2}{E^3}\widehat{L}_i(1)\ b^{\pm m,\mathrm{o}}_\ell, \tag{3.12}$$

for $0\leqslant i\leqslant N$ and $m\leqslant\ell\leqslant M_t$.

[2] Throughout the paper matrices and arrays will be denoted by capital letters while vectors will denoted by lower case letters.

The solution of the system can be calculated by factorisation and forward-backward substitutions for the symmetric matrix

$$\widehat{A}_\gamma \equiv \frac{1}{E^2}\widehat{D} + \gamma \widehat{M}. \tag{3.13}$$

Alternatively, we can also diagonalise this matrix, by considering the symmetric eigenvalue problem $\widehat{A}_\gamma \hat{w}_\gamma = \hat{\lambda}_\gamma \hat{w}_\gamma$ by employing, for instance, LAPACK Library [1]. The advantage of using the basis (3.5) is to give one and the same matrix $\widehat{A}_\gamma$ for all values of ℓ in the solution of Neumann problems in the spherical gap.

It is interesting to evaluate how the condition number of the system matrix in (3.7) depends on the basis degree. In Table 1 we report the condition numbers for several basis degrees for $\ell = 0$, with $E = \frac{1}{2}$, and for three different values of γ, $\gamma = 0$, 10^3, 10^6, as an example. Results show that, for low values of the γ parameter, the condition number behaviour is dominated by the stiffness matrix and grows as N^4, which is typical for spectral methods.

Convergence tests have been performed against analytical solutions evaluating the error in the $L^\infty(\Omega)$ norm as well as in the weighted $L^2_w(\Omega)$ norm, with weight $w(r,\theta) = r^2\sin^2\theta$, $L^2_w\text{error} = \|u_{\text{computed}} - u_{\text{exact}}\|_{L^2_w}$, where

$$\|u\|^2_{L^2_w} = \int_{r_\text{i}}^{r_\text{o}}\int_0^\pi\int_0^{2\pi} [u(r,\theta,\phi)]^2 r^2\,\mathrm{d}r\sin^2\theta\,\mathrm{d}\theta\,\mathrm{d}\phi. \tag{3.14}$$

All test problems are defined by exact solutions $u = u(x,y,z)$ which are expressed in terms of Cartesian coordinates to yield infinitely differentiable functions also on the z axis.

The exact solution for the Neumann problem with $\gamma = 1.5$ in a spherical gap $0.5 \leqslant r \leqslant 1.5$ is defined by $u = e^{p(x-x_0)^2+q(y-y_0)^2+z-z_0}$, with $p = 0.5$, $q = 1.2$ and $x_0 = 0.1$, $y_0 = 0.2$, $z_0 = 0.3$. The results reported in Table 2 show that the expected spectral convergence is attained.

The second test for the Neumann solver is the Poisson problem with exact solution $u = \sin x \sin y \sin z$ in the spherical gap $0.5 \leqslant r \leqslant 1$. Table 3 gives the L^∞ error of the approximate solutions provided by the proposed spectral algorithm and by hybrid methods of Lai et al., as well the Fishpack library [6], which both use spherical harmonics in the angular directions and second-order finite differences in the radial direction. The results show the second-order accuracy of the hybrid spectral/finite difference methods, to be compared with the spectral convergence of the proposed method.

3.2. Dirichlet problem

Let us now consider the case of Dirichlet boundary condition, which for the transformed unknowns $u^m_\ell(x)$ read $u^m_\ell(\mp 1) = a^{m,\text{i,o}}_\ell$, where m runs on positive and negative integers.

Table 1
Condition number of matrix in (3.7) with $\ell = 0$ and $E = \frac{1}{2}$ of the Neumann problem in a spherical gap for different basis degrees and γ values

N	16	32	64	128
$\gamma = 0$	9.0×10^3	1.3×10^5	1.9×10^6	3.0×10^7
$\gamma = 10^3$	1.6×10^2	2.2×10^3	3.2×10^4	5.0×10^5
$\gamma = 10^6$	8.1	1.2×10	6.8×10	9.4×10^2

Table 2
Neumann problem for Helmholtz operator with $\gamma = 1$ in the spherical gap $0.5 \leqslant r \leqslant 1.5$

$N = M_t$	L^∞ error	L^2_w error
10	7.4×10^{-3}	4.2×10^{-3}
15	1.9×10^{-5}	1.1×10^{-5}
20	2.2×10^{-8}	1.4×10^{-8}
25	2.5×10^{-11}	1.3×10^{-11}
30	9.9×10^{-12}	7.4×10^{-12}
35	9.9×10^{-12}	7.9×10^{-12}

Exact solution $u = e^{p(x-x_0)^2+q(y-y_0)^2+z-z_0}$ with $p = \frac{1}{2}$, $q = 1.2$ and $\mathbf{r}_0 = (0.1,0.2,0.3)$.

Table 3
L^∞ error for Poisson–Neumann problem in the spherical gap $0.5 \leqslant r \leqslant 1$

$N = M_t$	Present, spectral	Spectral/FD [6]	Fishpack
9	3.0×10^{-7}	3.7×10^{-3}	5.9×10^{-3}
16	4.3×10^{-13}	1.0×10^{-3}	1.2×10^{-3}
32	1.6×10^{-14}	2.5×10^{-4}	3.1×10^{-4}
64	8.4×10^{-14}	6.4×10^{-5}	7.8×10^{-5}

Exact solution $u = \sin x \sin y \sin z$.

The approximate solution $u_\ell^{\pm m}(x)$ of the Dirichlet problem is expanded in the series

$$u_\ell^{\pm m}(x) = \sum_{i=0}^{N} u_{\ell;i}^{\pm m} L_i^*(x), \tag{3.15}$$

where the elements of the basis $\{L_i^*(x)\}$ are defined as

$$L_0^*(x) = 1, \quad L_1^*(x) = \frac{x}{\sqrt{2}}, \quad L_i^*(x) = \frac{L_{i-2}(x) - L_i(x)}{\sqrt{2(2i-1)}}, \quad i \geqslant 2, \tag{3.16}$$

where $\{L_i(x), i = 0,1,2, \dots\}$ indicate Legendre polynomials. This basis is slightly more complicate than the one for the Neumann problem in that it contains linear combinations of two Legendre polynomials which vanish on the boundary to fulfill homogeneous Dirichlet conditions, as introduced by Shen [15]. The first two functions of the basis are here included to impose nonhomogeneous boundary values by means of a lifting.

The expansion coefficients of the solution $u_\ell^{\pm m}(x)$ are now taken as a *vector* unknown, $u_\ell^{\pm m} = \{u_{\ell;i}^{\pm m}, 0 \leqslant i \leqslant N\}$ [where the absence of the variable specification (x) in the vector quantity must be noticed] and similarly the expansion coefficients of the source term $g_\ell^{\pm m}(x)$ define the known vector $g_\ell^{\pm m} = \{g_{\ell;i}^{\pm m}, 0 \leqslant i \leqslant N\}$. Then, the linear system of equations can be written compactly in matrix form

$$\left[\frac{1}{E^2} D + \frac{\ell(\ell+1)}{E^2} M^0 + \gamma M\right] u_\ell^{\pm m} = g_\ell^{\pm m} + \langle \text{b.t.} \rangle_\ell^{\pm m}, \tag{3.17}$$

where the boundary term $\langle \text{b.t.} \rangle_\ell^{\pm m}$ will be made to disappear by enforcing the Dirichlet condition by means of a lifting of the nonhomogeneous boundary data, to be described below. The matrices D, M and M^0 corresponding to the operators acting on the radial coordinate are

$$\begin{aligned} D_{i,i'} &= \int_{-1}^{1} (\alpha + x)^2 \frac{\mathrm{d}L_i^*(x)}{\mathrm{d}x} \frac{\mathrm{d}L_{i'}^*(x)}{\mathrm{d}x} \mathrm{d}x, \\ M_{i,i'} &= \int_{-1}^{1} (\alpha + x)^2 L_i^*(x) L_{i'}^*(x)\ \mathrm{d}x, \\ M_{i,i'}^0 &= \int_{-1}^{1} L_i^*(x) L_{i'}^*(x)\ \mathrm{d}x, \end{aligned} \tag{3.18}$$

with $(i,i') \geqslant 0$. The matrices D, M and M^0 are banded symmetric and their nonzero elements can be evaluated exactly in closed form. The matrix D is penta-diagonal, according to the following profile

$$D = \begin{pmatrix} 0 & 0 & 0 & & & & \\ 0 & c_1 & b_1 & a_1 & & & \\ 0 & b_1 & c_2 & b_2 & a_2 & & \\ & a_1 & b_2 & \ddots & \ddots & \ddots & \\ & & a_2 & \ddots & \ddots & \ddots & a_{N-2} \\ & & & \ddots & \ddots & \ddots & b_{N-1} \\ & & & & a_{N-2} & b_{N-1} & c_N \end{pmatrix} \tag{3.19}$$

and its elements are defined by

$$\begin{aligned} a_1 &= \frac{-2}{3\sqrt{5}}, \qquad a_i = \frac{i(i+1)}{(2i+1)\sqrt{(2i+3)(2i-1)}}, \quad i \geqslant 2, \\ b_1 &= -\frac{2\alpha}{\sqrt{3}}, \quad b_i = 2\alpha\frac{i}{\sqrt{4i^2-1}}, \quad i \geqslant 2, \\ c_1 &= \alpha^2 + \frac{1}{3}, \quad c_i = \alpha^2 + \frac{2i^2-2i-1}{(2i-3)(2i+1)}, \quad i \geqslant 2. \end{aligned} \tag{3.20}$$

Matrix M has nine diagonals of nonzero elements, with the following pattern

$$M = \begin{pmatrix} \bar{e}_0 & \bar{d}_0 & \bar{c}_0 & \bar{b}_0 & \bar{a}_0 & & & \\ \bar{d}_0 & \bar{e}_1 & \bar{d}_1 & \bar{c}_1 & \bar{b}_1 & \bar{a}_1 & & \\ \bar{c}_0 & \bar{d}_1 & \ddots & \ddots & \ddots & \ddots & \ddots & \\ \bar{b}_0 & \bar{c}_1 & \ddots & \ddots & \ddots & \ddots & \ddots & \bar{a}_{N-4} \\ \bar{a}_0 & \bar{b}_1 & \ddots & \ddots & \ddots & \ddots & \ddots & \bar{b}_{N-3} \\ & \bar{a}_1 & \ddots & \ddots & \ddots & \ddots & \ddots & \bar{c}_{N-2} \\ & & \ddots & \ddots & \ddots & \ddots & \ddots & \bar{d}_{N-1} \\ & & & \bar{a}_{N-4} & \bar{b}_{N-3} & \bar{c}_{N-2} & \bar{d}_{N-1} & \bar{e}_N \end{pmatrix} \tag{3.21}$$

where, as shown in [3],

$$\begin{aligned} \bar{d}_0 &= 2\alpha\frac{\sqrt{2}}{3}, \qquad \bar{d}_1 = 2\alpha\frac{1}{5\sqrt{3}}, \quad \bar{d}_i = 2\alpha\frac{i}{(4i^2-9)\sqrt{4i^2-1}}, \quad i \geqslant 2, \\ \bar{b}_0 &= 2\alpha\frac{1}{3}\sqrt{\frac{2}{5}}, \quad \bar{b}_1 = 2\alpha\frac{2}{15\sqrt{7}}, \quad \bar{b}_i = 2\alpha\frac{-(i+1)}{(2i+1)(2i+3)\sqrt{(2i-1)(2i+5)}}, \quad i \geqslant 2, \end{aligned} \tag{3.22}$$

and

$$\begin{aligned} \bar{e}_0 &= 2\alpha^2 + \tfrac{2}{3}, & \bar{e}_1 &= \tfrac{\alpha^2}{3} + \tfrac{1}{5}, \\ \bar{c}_0 &= \sqrt{\tfrac{2}{3}}\alpha^2 + \tfrac{1}{5}\sqrt{\tfrac{2}{3}}, & \bar{c}_1 &= \tfrac{\alpha^2}{3\sqrt{5}} + \tfrac{1}{7\sqrt{5}}, \\ \bar{a}_0 &= \tfrac{2}{3\cdot 5}\sqrt{\tfrac{2}{7}}, & \bar{a}_1 &= \tfrac{2}{3\cdot 5\cdot 7}, \end{aligned} \tag{3.23}$$

while, for $i \geqslant 2$,

$$\begin{aligned} \bar{e}_i &= \frac{2}{(2i-3)(2i+1)}\left(\frac{i^2-i-3}{(2i-5)(2i+3)} + \alpha^2\right), \\ \bar{c}_i &= \frac{1}{(2i+1)\sqrt{(2i-1)(2i+3)}}\left(\frac{3}{(2i-3)(2i+5)} - \alpha^2\right), \\ \bar{a}_i &= -\frac{(i+1)(i+2)}{(2i+1)(2i+3)(2i+5)\sqrt{(2i-1)(2i+7)}}. \end{aligned} \tag{3.24}$$

Matrix M^0 is obtained from the contribution to the M matrix which is proportional to α^2, see also [14].

Finally, we have

$$g^{\pm m}_{\ell;i} = \int_{-1}^{1} L^*_i(x)(\alpha + x)^2 g^{\pm m}_{\ell}(r(x))\, \mathrm{d}x, \tag{3.25}$$

for $0 \leqslant i \leqslant N$ and $m \leqslant \ell \leqslant M_t$. The integrals are evaluated numerically by Gauss–Legendre formula with $N + 2$ integration points.

3.2.1. Lifting of the nonhomogeneous boundary condition

The nonhomogeneous Dirichlet boundary condition is imposed by means of a lifting.This is achieved by decomposing the solution in two parts, as follows,

$$u_\ell^{\pm m}(x) = u_{\ell;a}^{\pm m}(x) + u_{\ell;\mathrm{hom}}^{\pm m}(x), \tag{3.26}$$

where

$$u_{\ell;a}^{\pm m}(x) = \frac{1}{2}\left(a_\ell^{\pm m,\mathrm{i}} + a_\ell^{\pm m,\mathrm{o}}\right) + \frac{1}{2}\left(a_\ell^{\pm m,\mathrm{o}} - a_\ell^{\pm m,\mathrm{i}}\right)x \tag{3.27}$$

while the part of the solution satisfying homogeneous conditions is given by the reduced summation:

$$u_{\ell;\mathrm{hom}}^{\pm m}(x) = \sum_{i=2}^{N} u_{\ell;i}^{\pm m} L_i^*(x). \tag{3.28}$$

Then, one defines the matrix

$$A_{(\ell)} = \frac{1}{E^2}D + \frac{\ell(\ell+1)}{E^2}M^0 + \gamma M \tag{3.29}$$

and introduces its partitioning to separate the "internal" component[3] $\mathsf{A}_{(\ell)}$, with elements $a_{i,i'}$ such that $2 \leqslant (i,i') \leqslant N$, from the two-column array

$$A_{(\ell)}^s = \{a_{i,i'}, i = 2,3,\ldots,N; i' = 0,1\}. \tag{3.30}$$

The same partitioning is applied to the unknown vector $\{u_{\ell,i}^{\pm m}, i = 0,1,\ldots,N\}$ to isolate the degrees of freedom associated with the boundary values

$$u_{\ell;a}^{\pm m,s} = \left\{\frac{1}{2}\left(a_\ell^{\pm m,\mathrm{i}} + a_\ell^{\pm m,\mathrm{o}}\right), \frac{1}{\sqrt{2}}\left(a_\ell^{\pm m,\mathrm{o}} - a_\ell^{\pm m,\mathrm{i}}\right)\right\}. \tag{3.31}$$

from vector $\mathsf{u}_\ell^{\pm m} = \{u_{\ell,i}^{\pm m}, i = 2,3,\ldots,N\}$ of the "internal" degrees of freedom. According to this partitioning the lifted linear system will be

$$\mathsf{A}_{(\ell)}\mathsf{u}_\ell^{\pm m} = \mathsf{g}_\ell^{\pm m} - A_{(\ell)}^s u_{\ell;a}^{\pm m,s}, \tag{3.32}$$

where $\mathsf{A}_{(\ell)} \equiv \frac{1}{E^2}\mathsf{D} + \frac{\ell(\ell+1)}{E^2}\mathsf{M}^0 + \gamma\mathsf{M}$. We solve this linear system by Cholesky factorisation and substitutions for a band symmetric matrix with nine diagonals.

In Table 4 we report the condition numbers of matrix $\mathsf{A}_{(\ell)}$ for $\ell = 0$ of the Dirichlet solver for several basis degrees and $E = \frac{1}{2}$, for three different values of γ, $\gamma = 1$, 10^3, 10^6. Results show the very good conditioning of Shen's basis. This basis is better conditioned than the one employed for the Neumann problem. Its use is less efficient, especially when a single equation has to be solved, but could become mandatory when very high resolutions are needed.

The Dirichlet spectral solver has been tested against the same test exact solution considered for the Neumann problem, with $\gamma = 2$ and in the same spherical gap $0.5 \leqslant r \leqslant 1.5$. Table 5 shows the spectral convergence of the method. The greater accuracy of the Dirichlet solver with respect to the Neumann solver in both norms, cf. Table 2, is related to a better conditioning of the matrices for the Dirichlet boundary value problem.

Also the Dirichlet spectral solver is compared with hybrid spectral/difference methods of [6] and the Fishpack algorithm, on the Poisson problem with exact solution $u = \sin x \sin y \sin z$ in the spherical gap $0.5 \leqslant r \leqslant 1$. Table 6 gives the L^∞ errors of the three methods, which confirm the spectral convergence of the fully spectral solvers versus second-order accuracy of hybrid spectral/finite difference methods.

[3] In the following, sanserif characters will be used to denote matrices and vectors pertaining to the reduced problem after the lifting for the nonhomogeneous boundary conditions.

Table 4
Condition number of matrix in (3.32) with $\ell = 0$ and $E = \frac{1}{2}$ of the Dirichlet problem in a spherical gap for different basis degrees and γ values

N	16	32	64	128
$\gamma = 1$	8.6	8.9	9.0	9.0
$\gamma = 10^3$	3.6×10^2	4.2×10^2	4.4×10^2	4.4×10^2
$\gamma = 10^6$	3.0×10^3	4.3×10^4	2.7×10^5	4.2×10^5

Table 5
Dirichlet problem for Helmholtz operator with $\gamma = 2$ in the spherical gap $0.5 \leqslant r \leqslant 1.5$

$N = M_t$	L^∞ error	L^2_w error
20	2.2×10^{-8}	1.4×10^{-8}
30	1.8×10^{-13}	7.6×10^{-14}
40	2.2×10^{-12}	4.2×10^{-13}

Exact solution $u = e^{p(x-x_0)^2+q(y-y_0)^2+z-z_0}$ with $p = \frac{1}{2}$, $q = 1.2$ and $\boldsymbol{r}_0 = (0.1, 0.2, 0.3)$.

Table 6
L^∞ error for Poisson–Dirichlet problem in the spherical gap $0.5 \leqslant r \leqslant 1$

$N = M_t$	Present, spectral	Spectral/FD [6]	Fishpack
8	9.3×10^{-7}	1.3×10^{-3}	1.8×10^{-3}
16	5.2×10^{-16}	3.9×10^{-4}	4.6×10^{-4}
32	6.5×10^{-16}	1.0×10^{-4}	1.1×10^{-4}
64	1.2×10^{-15}	2.5×10^{-5}	2.9×10^{-5}

Exact solution $u = \sin x \sin y \sin z$.

4. Sphere

The Helmholtz equations is now solved within the sphere of radius $r = c$, so that the domain contains the polar axis as well as the center of the sphere.

Let us introduce the dimensionless radial variable $\rho = r/c$, ranging in the unit interval $0 < \rho \leqslant 1$. The ordinary differential equation for the unknown $u^m_\ell(\rho)$ will become

$$-\frac{\mathrm{d}}{\mathrm{d}\rho}\left(\rho^2 \frac{\mathrm{d}u^m_\ell}{\mathrm{d}\rho}\right) + [\ell(\ell+1) + \gamma\rho^2]u^m_\ell = \rho^2 g^m_\ell(\rho). \tag{4.1}$$

for $m = 0, \pm 1, \pm 2, \ldots, \pm(M_t - 1), M_t$, and $\ell = |m|, |m|+1, \ldots, M_t$. Here the original constant γ of the Helmholtz equation has been redefined by a multiplication by c^2. The weak form of this modal equation for $u^m_\ell = u^m_\ell(\rho)$ is obtained by multiplying the equation by suitable functions $v(\rho)$ and integrating over the interval [0,1]. An integration by parts gives

$$\int_0^1 \left\{\rho^2 \frac{\mathrm{d}v}{\mathrm{d}\rho}\frac{\mathrm{d}u^m_\ell}{\mathrm{d}\rho} + [\ell(\ell+1) + \gamma\rho^2]v u^m_\ell\right\}\mathrm{d}\rho = \int_0^1 \rho^2 v(\rho)\ g^m_\ell(\rho)\ \mathrm{d}\rho + v(1)\frac{\mathrm{d}u^m_\ell(1)}{\mathrm{d}\rho}. \tag{4.2}$$

It can be noted that the left contribution of the boundary term disappears since $\rho = 0$ at the sphere center.

The condition of infinite differentiability of u up to the sphere centre implies the following conditions on the modal expansion coefficients: $u^{\pm m}_\ell(\rho) \sim \rho^\ell U(\rho^2)$ as $\rho \to 0$. This constraint allows one to expand the solution $u^{\pm m}_\ell(\rho)$ in the following series

$$u^{\pm m}_\ell(\rho) = \sum_{i=\ell}^{M_t} u^{\pm m}_{\ell;i} \rho^\ell P^{\bigstar \ell+\frac{1}{2}}_{i-\ell}(2\rho^2 - 1). \tag{4.3}$$

The basis functions $P^{\bigstar \ell+\frac{1}{2}}_{i-\ell}(s)$ are defined in terms of Jacobi polynomials $P^{(\alpha,\beta)}_k(s)$, $-1 \leqslant s \leqslant 1$, by relations:

$$P^{\bigstar \ell+\frac{1}{2}}_0(s) = 1 \quad \text{and} \quad P^{\bigstar \ell+\frac{1}{2}}_k(s) = \frac{1-s}{2} P^{(1,\ell+\frac{1}{2})}_{k-1}(s), \quad k = 1, 2, \ldots. \tag{4.4}$$

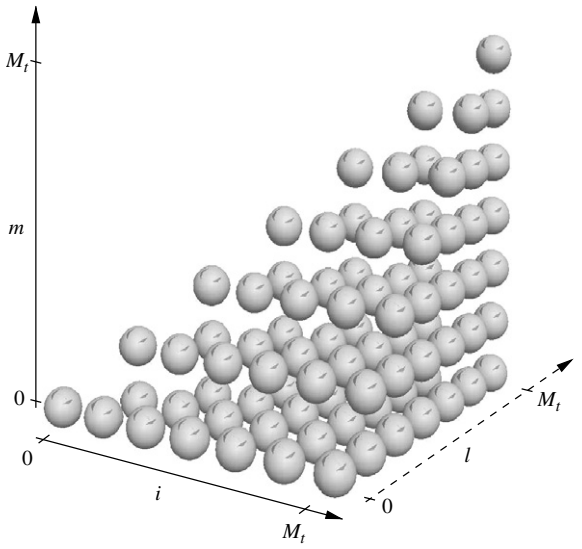

Fig. 1. Schematic of the data structure of the expansion coefficients (cosine part) in 3D elliptic problem in a sphere for $M_t = 6$.

In Fig. 1 a picture of the set of spectral coefficients used to represent a function in a sphere is given for $M_t = 6$: only the coefficients with $m \geqslant 0$ are considered. In general, the total number of cosine and sine expansion coefficients is equal to $\frac{1}{6}(M_t+1)(2M_t^2+7M_t+6)$. This value represents the minimum number of degrees of freedom necessary to assure spectral accuracy in the solution of Helmholtz equation in a sphere.

The complete spectral expansion considered here for the unknown $u(\rho,\theta,\phi)$ of the elliptic boundary value problem in the spherical domain is therefore given by

$$\begin{aligned} u(\rho,\theta,\phi) = & \sum_{\ell=0}^{M_t}\left[\sum_{i=\ell}^{M_t} u^0_{\ell;i}\rho^\ell P^{\star\ell+\frac{1}{2}}_{i-\ell}(2\rho^2-1)\right]\widehat{P}^0_\ell(\cos\theta) \\ & + 2\left\{\sum_{\ell=m}^{M_t}\left[\sum_{i=\ell}^{M_t} u^{\pm m}_{\ell;i}\rho^\ell P^{\star\ell+\frac{1}{2}}_{i-\ell}(2\rho^2-1)\right]\widehat{P}^{|m|}_\ell(\cos\theta)\right\}\begin{matrix}\cos(m\phi)\\ -\sin(m\phi)\end{matrix}\sum_{m=1}^{M_t-1} \\ & + u^{M_t}_{M_t;M_t}\rho^{M_t}\widehat{P}^{M_t}_{M_t}(\cos\theta)\cos(M_t\phi), \end{aligned} \tag{4.5}$$

where the equality of the upper extremes of the three summations, as well as the nested dependence of the lower extremes in the double and triple summations can be noticed.

The approximate version of the weak problem for $u^{\pm m}_\ell(\rho)$ assumes the following matrix form

$$[D_{\boxed{\ell}} + \gamma M_{\boxed{\ell}}]u^{\pm m}_{\boxed{\ell}} = g^{\pm m}_{\boxed{\ell}} + \langle \text{b.t.}\rangle^{\pm m}_{\boxed{\ell}}, \tag{4.6}$$

where the special index notation $\boxed{\ell}$ is used to emphasise that the order of the (square) matrices and of the vectors depends on the summation index ℓ. More precisely, the order corresponding to $\boxed{\ell}$ is $M_t - \ell + 1$, and therefore runs from the maximum order $M_t + 1$ for $\ell = 0$, to the minimum order *1* for $\ell = M_t$.

The matrices $D_{\boxed{\ell}}$ and $M_{\boxed{\ell}}$ corresponding to the operators on the radial coordinate are

$$\begin{aligned} D_{\boxed{\ell}\,i,i'} = & \int_{-1}^{1}\left\{4\left(\frac{1+s}{2}\right)^{\frac{3}{2}}\frac{\mathrm{d}}{\mathrm{d}s}\left[\left(\frac{1+s}{2}\right)^{\frac{\ell}{2}}P^{\star\ell+\frac{1}{2}}_{i-\ell}(s)\right]\frac{\mathrm{d}}{\mathrm{d}s}\left[\left(\frac{1+s}{2}\right)^{\frac{\ell}{2}}P^{\star\ell+\frac{1}{2}}_{i'-\ell}(s)\right] + \frac{\ell(\ell+1)}{4}\right. \\ & \left.\times\left(\frac{1+s}{2}\right)^{\ell-\frac{1}{2}}P^{\star\ell+\frac{1}{2}}_{i-\ell}(s)P^{\star\ell+\frac{1}{2}}_{i'-\ell}(s)\right\}\mathrm{d}s, \\ M_{\boxed{\ell}\,i,i'} = & \frac{1}{4}\int_{-1}^{1}\left(\frac{1+s}{2}\right)^{\ell+\frac{1}{2}}P^{\star\ell+\frac{1}{2}}_{i-\ell}(s)P^{\star\ell+\frac{1}{2}}_{i'-\ell}(s)\ \mathrm{d}s, \end{aligned} \tag{4.7}$$

Table 7
Convergence properties of the mass matrix problem for the basis (4.4) on the oscillatory solution $u = \sin[20(x - x_0)^2 + 4(y - y_0)^2 + z - z_0]$ with $\boldsymbol{r}_0 = (0.1, 0.2, 0.3)$

M_t	L^∞ error	L^2_w error
32	1.56	4.87
64	1.54	4.05
96	0.93	1.25
128	0.93×10^{-3}	0.59×10^{-3}
192	2.10×10^{-11}	3.83×10^{-12}
224	4.18×10^{-11}	5.91×10^{-12}
256	1.00×10^{-10}	1.22×10^{-11}

for $\ell \leqslant (i,i') \leqslant M_t$. Matrix $D_{[\ell]}$ is diagonal and matrix $M_{[\ell]}$ is tridiagonal. Their nonzero elements are obtained by numerical evaluation of the integrals by means of Gauss–Jacobi formula with $M_t + 1$ integration points, namely,

$$\int_{-1}^{1} \sqrt{1+s}\, f(s)\, \mathrm{d}s = \sum_{j=1}^{M_t+1} f(s_j)\, \omega_j, \tag{4.8}$$

where s_j and ω_j are the quadrature points and weights associated with the Jacobi polynomial $P_k^{(0,\frac{1}{2})}(s)$.

As far as the right-hand side is concerned, the components of the source vector and of the boundary term are

$$g^{\pm m}_{[\ell]\, i} = \frac{1}{4} \int_{-1}^{1} \left(\frac{1+s}{2}\right)^{\frac{\ell+1}{2}} P^{\star \ell+\frac{1}{2}}_{i-\ell}(s)\; g^{\pm m}_{\ell}\left(\left(\frac{1+s}{2}\right)^{1/2}\right) \mathrm{d}s, \tag{4.9}$$

$$\langle \text{b.t.} \rangle^{\pm m}_{[\ell]\, i} = P^{\star \ell+\frac{1}{2}}_{i-\ell}(1)\; b^{\pm m}_{\ell}, \tag{4.10}$$

for $m \leqslant \ell \leqslant M_t$ and $\ell \leqslant i \leqslant M_t$. The integrals above are evaluated by the same Gauss–Jacobi formula.

The basis (4.4) does not suffer from the bad conditioning typically encountered by other bases used to approximate functions that behave analytically at the center in spherical coordinates or on the axis in cylindrical ones.The conditioning of the new basis is assessed by solving the mass matrix problem with a strongly oscillatory solution $u = \sin[h(x - x_0)^2 + k(y - y_0)^2 + z - z_0]$ for $h = 20$, $k = 40$ and $\boldsymbol{r}_0 = (0.1,0.2,0.3)$. The numerical errors are reported in Table 7. They show the high number of polynomials required to resolve the oscillations and, once the resolution is adequate, the spectral accuracy which, also by virtue of the tridiagonal mass matrix, is not jeopardised by the confinement near $\rho = 1$ of the nonvanishing region of the polynomials for large ℓ. In short, the proposed basis turns out to be well conditioned.

4.1. Neumann problem

Let us first consider the case of a Neumann boundary condition on the surface of the sphere: $\frac{\partial u(1,\theta,\phi)}{\partial \rho} = b(\theta,\phi)$, where $b(\theta,\phi)$ is the boundary value of u on the surface $\rho = 1$. If $\gamma = 0$, the data of the Neumann problem, i.e., the source term f and the boundary values b should satisfy the following compatibility condition $\int_\Omega f = -\int_{\partial\Omega} b$, Ω being the spherical domain, under which the solution is defined up to an additive constant.

After the transformation to the associated Legendre functions, each expansion coefficient $u^m_\ell(\rho)$, with $m = 0, \pm 1, \pm 2, \ldots, \pm(M_t - 1), M_t$, and $\ell = |m|, |m| + 1, \ldots, M_t$, will be supplemented by the derivative condition: $\frac{\mathrm{d}u^m_\ell(1)}{\mathrm{d}\rho} = b^m_\ell$. Incorporating the derivative boundary value, the weak modal equation for the Neumann problem will be Eq. (4.2) with the replacement of the last term on the right-hand side by $v(1)b^m_\ell$.

Thus, the Neumann problem within a sphere leads to the linear system (4.6) for the unknown $u^{\pm m}_{[\ell]}$, with the tridiagonal matrix

$$A_{[\ell]} = D_{[\ell]} + \gamma M_{[\ell]}. \tag{4.11}$$

Table 8
Condition number for matrix in (4.11) with $\ell = 0$ of the Neumann problem in a sphere for different basis degrees and γ values

N	16	32	64	128
$\gamma = 0$	1.9×10	3.9×10	7.9×10	1.5×10^2
$\gamma = 10^3$	1.6×10^2	1.6×10^2	1.6×10^2	1.6×10^2
$\gamma = 10^6$	8.8×10^3	2.5×10^4	2.5×10^4	2.7×10^4

Table 9
Neumann problem for Helmholtz operator with $\gamma = 2$ in the sphere $\rho \leqslant 1$

M_t	L^∞ error	relative L^2_w error
10	2.8×10	1.0×10^{-2}
20	8.3×10^{-3}	2.1×10^{-6}
30	2.3×10^{-7}	4.7×10^{-11}
40	1.3×10^{-10}	8.1×10^{-14}

Exact solution $u = e^{p(x-x_0)^2+q(y-y_0)^2+z-z_0}$ with $p = 3$, $q = 6$ and $\mathbf{r}_0 = (0.1, 0.2, 0.3)$.

The solution of the system is obtained by LDL^T factorisation and substitutions tailored to tridiagonal matrices.

Also for the spherical domain it is worthwhile to evaluate the condition number of the system matrix $A_{\boxed{\ell}}$ as a function of basis degree and γ, see Table 8. For the Neumann boundary value problem one has to consider also the minimum value of $\gamma = 0$, which is encountered in the solution of a Poisson equation (occurring, for instance, when the Navier–Stokes equations are solved by means of a projection method). In this case the condition number increases quite slowly with the polynomial degree, leading to well conditioned system matrices.

The L^∞ and L^2_w errors for the solution of the Neumann problem with $\gamma = 2$, $p = 3$ and $q = 6$ in the unit sphere $\rho \leqslant 1$ are reported in Table 9. They demonstrate that spectral convergence is achieved with an accuracy very similar to that reached in the spherical gap, cf. with results in Table 2.

4.2. Dirichlet problem

Let us now assume a Dirichlet condition $u_{|\rho=1} = a(\theta,\phi)$, where function $a(\theta,\phi)$ represents the boundary value specified on the spherical surface $\rho = 1$. After introducing the expansion of the boundary data in trigonometric and associated Legendre functions, we obtained the modal condition

$$u^m_\ell(1) = a^m_\ell, \tag{4.12}$$

for $\ell = |m|, |m| + 1, \ldots, M_t$ with $m = 0, \pm 1, \pm 2, \ldots$

Considering now the modal unknown $u^{\pm m}_\ell(\rho)$, the approximate solution is expanded as in (4.3) and the weak equation for the radial Dirichlet problem of each modal unknown reads as system (4.6). However, in the Dirichlet case the boundary term $\langle \text{b.t.} \rangle^{\pm m}_{\boxed{\ell}}$ will be made to disappear by enforcing the nonzero boundary values by means of a lifting of each modal datum, to be described below.

4.2.1. Lifting of the nonhomogeneous boundary value

The nonzero Dirichlet boundary condition is imposed by means of lifting, which consists in decomposing the solution in two parts, as follows,

$$u^{\pm m}_\ell(\rho) = a^{\pm m}_\ell + u^{\pm m}_{\ell;\mathrm{hom}}(\rho), \tag{4.13}$$

where the part of the solution satisfying the homogeneous condition is expressed by the reduced summation

$$u^{\pm m}_{\ell;\mathrm{hom}}(\rho) = \sum_{i=\ell+1}^{M_t} u^{\pm m}_{\ell;i} \rho^\ell P^{\bigstar \ell+\frac{1}{2}}_{i-\ell}(2\rho^2 - 1), \tag{4.14}$$

where the absence of the first term with $i = \ell$ must be noticed.Then, one consider matrix $A_{\boxed{\ell}} = D_{\boxed{\ell}} + \gamma M_{\boxed{\ell}}$ and introduces its partitioning to separate the "internal" component $\mathsf{A}_{\boxed{\ell}}$, with elements $a_{i,i'}$ such that $\ell + 1 \leqslant (i,i') \leqslant M_t$, from its first column

Table 10
Condition number for matrix in (4.16) with $\ell = 0$ of the Dirichlet problem in a sphere for different basis degrees and γ values

N	16	32	64	128
$\gamma = 1$	1.6×10	3.2×10	6.6×10	1.3×10^2
$\gamma = 10^3$	2.5×10	2.5×10	2.5×10	2.5×10
$\gamma = 10^6$	3.1×10^2	1.8×10^3	4.1×10^3	4.1×10^3

Table 11
Dirichlet problem for Helmholtz operator with $\gamma = 2$ in the sphere $\rho \leqslant 1$

M_t	L^∞ error	Relative L^2_w error
10	2.7×10	1.0×10^{-2}
20	8.3×10^{-3}	2.1×10^{-6}
30	2.3×10^{-7}	4.7×10^{-11}
40	2.0×10^{-11}	3.0×10^{-15}
50	2.5×10^{-11}	8.4×10^{-15}

Exact solution $u = e^{p(x-x_0)^2+q(y-y_0)^2+z-z_0}$ with $p = 3$, $q = 6$ and $\boldsymbol{r}_0 = (0.1, 0.2, 0.3)$.

$$A^s_{[\ell]} = \{a_{i,\ell}, i = \ell+1, \ell+2, \ldots, M_t\}, \tag{4.15}$$

with the first diagonal element eliminated. The same partitioning is applied to the unknown vector $u^{\pm m}_{[\ell]} = \{u^{\pm m}_{[\ell]}, i = \ell, \ell+1, \ldots, M_t\}$ to isolate the "internal" degrees of freedom $\mathsf{u}^{\pm m}_{[\ell]} = \{u^{\pm m}_{[\ell]i}, i = \ell+1, \ell+2, \ldots, M_t\}$ from that associated with the boundary value $a^{\pm m}_\ell$ which defines the single component column vector $a^{\pm m}_{[\ell]} = \{a^{\pm m}_\ell\}$. According to this partitioning the lifted linear system will be

$$\mathsf{A}_{[\ell]}\mathsf{u}^{\pm m}_{[\ell]} = \mathsf{g}^{\pm m}_{[\ell]} - A^s_{[\ell]} a^{\pm m}_{[\ell]}, \tag{4.16}$$

where $\mathsf{A}_{[\ell]} \equiv \mathsf{D}_{[\ell]} + \gamma \mathsf{M}_{[\ell]}$. There is a subtlety in the use of the index notation $_{[\ell]}$ for the matrix $\mathsf{A}_{[\ell]}$ of the lifted problem. The order of this matrix is $M_t - \ell$, i.e., one unit less than the order of its parent matrix $A_{[\ell]}$, since the first component has been eliminated in the lifting. This implies that in the last problems for $\ell = M_t$ matrix $\mathsf{A}_{[\ell]}$ will not exist and the solution of the problem for these modes will consist only in taking into account the boundary values $a^{\pm m}_{M_t}$. The linear system of the lifted equations is solved by LDL^T factorisation algorithm, as in the Neumann case.

The condition numbers of the spectral matrices $\mathsf{A}_{[\ell]}$, for $\ell = 0$, for the radial discretisation of the elliptic problem with Dirichlet condition are also provided, for several basis degrees and γ values, see Table 10. As expected, its behaviour is very similar to that observed for the Neumann case reported in Table 8.

The results of the Helmholtz solver with $\gamma = 1$ for the Dirichlet problem in the unit sphere $\rho \leqslant 1$ are shown in Table 11 and demonstrate the spectral accuracy of the proposed method.

5. Vector elliptic equation in spherical components

5.1. Dirichlet problem for a vector field

We are now ready for the most interesting case, i.e., the three-dimensional vector Poisson equation $-\nabla^2 \boldsymbol{u} = \boldsymbol{f}(r,\theta,\phi)$ or Helmholtz equation $(-\nabla^2 + \gamma)\boldsymbol{u} = \boldsymbol{f}(r,\theta,\phi)$ in spherical coordinates (r,θ,ϕ), supplemented by the Dirichlet condition $\boldsymbol{u}_{|r=r_{\mathrm{i,o}}} = \boldsymbol{a}^{\mathrm{i,o}}(\theta,\phi)$.

When the Laplacian acts on a vector field $\boldsymbol{u}$ expressed in terms of its spherical coordinates u^r, u^θ and u^ϕ, the following matrix differential operator has to be considered

$$\mathbf{V}^2 = \begin{pmatrix} \nabla^2 - \frac{2}{r^2} & -\frac{2}{r^2 \sin\theta}\frac{\partial}{\partial\theta}(\sin\theta \ldots) & -\frac{2}{r^2 \sin\theta}\frac{\partial}{\partial\phi} \\ \frac{2}{r^2}\frac{\partial}{\partial\theta} & \nabla^2 - \frac{1}{r^2 \sin^2\theta} & -\frac{2\cos\theta}{r^2 \sin^2\theta}\frac{\partial}{\partial\phi} \\ \frac{2}{r^2 \sin\theta}\frac{\partial}{\partial\phi} & \frac{2\cos\theta}{r^2 \sin^2\theta}\frac{\partial}{\partial\phi} & \nabla^2 - \frac{1}{r^2 \sin^2\theta} \end{pmatrix}, \tag{5.1}$$

where the scalar spherical Laplace operator is defined in (2.2).

Being interested in purely real vector fields, let us now represent the dependence on the cyclic coordinate ϕ by means of the real Fourier series

$$\boldsymbol{u}(r,\theta,\phi) = \boldsymbol{u}_0(r,\theta) + 2\sum_{m=1}^{\infty}[\boldsymbol{u}_m(r,\theta)\cos(m\phi) - \boldsymbol{u}_{-m}(r,\theta)\sin(m\phi)], \tag{5.2}$$

where $\boldsymbol{u}_m(r,\theta) = u_m^r(r,\theta)\hat{\boldsymbol{r}} + u_m^\theta(r,\theta)\hat{\boldsymbol{\theta}} + u_m^\phi(r,\theta)\hat{\boldsymbol{\phi}}$, $-\infty < m < \infty$ with $\hat{\boldsymbol{r}}$, $\hat{\boldsymbol{\theta}}$ and $\hat{\boldsymbol{\phi}}$ denoting the unit vectors of the spherical coordinate system.

By virtue of the adopted Fourier expansion, the operator representing the Laplace operator ∇^2 in the space of the Fourier coefficients of a scalar function is

$$\eth_m^2 = \frac{1}{r^2}\frac{\partial}{\partial r}\left(r^2\frac{\partial}{\partial r}\right) + \frac{1}{r^2\sin\theta}\frac{\partial}{\partial\theta}\left(\sin\theta\frac{\partial}{\partial\theta}\right) - \frac{m^2}{r^2\sin^2\theta}, \tag{5.3}$$

whereas the operator representing the Laplace matrix operator $\mathbf{\nabla}^2$ in the space of the Fourier coefficients of a vector field is

$$\boldsymbol{\eth}_m^2 = \begin{pmatrix} \eth_m^2 - \frac{2}{r^2} & -\frac{2}{r^2\sin\theta}\frac{\partial}{\partial\theta}(\sin\theta\ldots) & \frac{2m}{r^2\sin\theta} \\ \frac{2}{r^2}\frac{\partial}{\partial\theta} & \eth_m^2 - \frac{1}{r^2\sin^2\theta} & \frac{2m\cos\theta}{r^2\sin^2\theta} \\ \frac{2m}{r^2\sin\theta} & \frac{2m\cos\theta}{r^2\sin^2\theta} & \eth_m^2 - \frac{1}{r^2\sin^2\theta} \end{pmatrix}. \tag{5.4}$$

The equation system for the coefficients of the m-th Fourier mode reads

$$-\boldsymbol{\eth}_m^2\begin{pmatrix} u_m^r \\ u_m^\theta \\ u_{-m}^\phi \end{pmatrix} = \begin{pmatrix} f_m^r(r,\theta) \\ f_m^\theta(r,\theta) \\ f_{-m}^\phi(r,\theta) \end{pmatrix} \tag{5.5}$$

Thus, for $m \neq 0$ the three spherical components of the vector Fourier mode are coupled together, while for the first mode $m = 0$ only the two components u_0^r and u_0^θ are coupled together.

5.2. Uncoupling the spherical vector components

We now describe a method originally proposed in [13] for uncoupling the three equations for the Fourier spherical components of the vector unknown by means of a suitable similarity transformation. The similarity transformation is constructed in two steps: first, the coupling between the r and θ components due to the off-diagonal terms containing the first-order derivative $\frac{\partial}{\partial\theta}$ is eliminated; then, the remaining coupling between the first new variable and the third unchanged variable (the ϕ component) is eliminated by means of the same similarity transformation considered in the analysis of the cylindrical coordinates.

Let us consider the first change of variables defined by the linear transformation

$$\boldsymbol{\Theta}_0 = \begin{pmatrix} \sin\theta & \cos\theta & 0 \\ \cos\theta & -\sin\theta & 0 \\ 0 & 0 & 1 \end{pmatrix}, \qquad \begin{pmatrix} \overline{u}_m^1 \\ \overline{u}_m^2 \\ u_{-m}^\phi \end{pmatrix} = \boldsymbol{\Theta}_0\begin{pmatrix} u_m^r \\ u_m^\theta \\ u_{-m}^\phi \end{pmatrix}. \tag{5.6}$$

Matrix $\boldsymbol{\Theta}_0$ is such that $\boldsymbol{\Theta}_0 = \boldsymbol{\Theta}_0^T = \boldsymbol{\Theta}_0^{-1}$. Furthermore, by standard calculations, it is possible to show that the similarity transformation provided by matrix $\boldsymbol{\Theta}_0$ gives the following partial diagonalisation of the matrix operator $\boldsymbol{\eth}_m^2$:

$$\boldsymbol{\Theta}_0\boldsymbol{\eth}_m^2\boldsymbol{\Theta}_0 = \begin{pmatrix} \eth_m^2 - \frac{1}{r^2\sin^2\theta} & 0 & \frac{2m}{r^2\sin^2\theta} \\ 0 & \eth_m^2 & 0 \\ \frac{2m}{r^2\sin^2\theta} & 0 & \eth_m^2 - \frac{1}{r^2\sin^2\theta} \end{pmatrix}. \tag{5.7}$$

It is important to note that this demonstration is relatively elaborated because of the presence of the function $\sin\theta$ inside and outside the derivative $\frac{\partial}{\partial\theta}$ in the operator $\eth_m^2$ as well as in its matrix counterpart $\boldsymbol{\eth}_m^2$.

Very easy is the elimination of the coupling still remaining between the first (new) and the third (old) components of the vector mode. Thus, introducing a second linear transformation defined by the matrix

$$\boldsymbol{Q} = \frac{1}{\sqrt{2}} \begin{pmatrix} 1 & 0 & 1 \\ 0 & \sqrt{2} & 0 \\ 1 & 0 & -1 \end{pmatrix}, \qquad \begin{pmatrix} u^1_{m-1} \\ u^2_m \\ u^3_{m+1} \end{pmatrix} = \boldsymbol{Q} \begin{pmatrix} \overline{u}^1_m \\ \overline{u}^2_m \\ u^\phi_{-m} \end{pmatrix}, \tag{5.8}$$

with, as before, $\boldsymbol{Q} = \boldsymbol{Q}^T = \boldsymbol{Q}^{-1}$, one obtains immediately $\boldsymbol{Q}\boldsymbol{\Theta}_0\boldsymbol{\partial}^2_m\Theta_0\boldsymbol{Q} = \mathrm{diag}(\partial^2_{m-1}, \partial^2_m, \partial^2_{m+1})$. Therefore, defining the complete transformation

$$\boldsymbol{\Theta} \equiv \boldsymbol{Q}\boldsymbol{\Theta}_0, \tag{5.9}$$

it is immediate to obtain

$$\boldsymbol{\Theta} = \frac{1}{\sqrt{2}} \begin{pmatrix} \sin\theta & \cos\theta & 1 \\ \sqrt{2}\cos\theta & -\sqrt{2}\sin\theta & 0 \\ \sin\theta & \cos\theta & -1 \end{pmatrix}, \begin{pmatrix} u^1_{m-1} \\ u^2_m \\ u^3_{m+1} \end{pmatrix} = \boldsymbol{\Theta} \begin{pmatrix} u^r_m \\ u^\theta_m \\ u^\phi_{-m} \end{pmatrix}. \tag{5.10}$$

The transformation $\boldsymbol{\Theta}$ is orthogonal. In fact $\boldsymbol{\Theta} = \boldsymbol{Q}\,\boldsymbol{\Theta}_0 = \boldsymbol{Q}^T\boldsymbol{\Theta}_0^T = [\boldsymbol{\Theta}_0\boldsymbol{Q}]^T$, since the matrices $\boldsymbol{\Theta}_0$ and $\boldsymbol{Q}$ are symmetric. But $\boldsymbol{\Theta}_0^{-1} = \boldsymbol{\Theta}_0$ and $\boldsymbol{Q}^{-1} = \boldsymbol{Q}$, so that $\boldsymbol{\Theta}_0\boldsymbol{Q} = \boldsymbol{\Theta}_0^{-1}\boldsymbol{Q}^{-1} = [\boldsymbol{Q}\boldsymbol{\Theta}_0]^{-1} = \boldsymbol{\Theta}^{-1}$. It follows that $\boldsymbol{\Theta}^T = \boldsymbol{\Theta}^{-1}$. Notice however that $\boldsymbol{\Theta} \neq \boldsymbol{\Theta}^T$ since $\boldsymbol{Q}$ and $\boldsymbol{\Theta}_0$ in general do not commute (except when $\theta = \pi/2$). So the previous complete diagonalisation of the matrix operator $\boldsymbol{\partial}^2_m$ can be written as

$$\boldsymbol{\Theta}\boldsymbol{\partial}^2_m\boldsymbol{\Theta}^T = \begin{pmatrix} \partial^2_{m-1} & 0 & 0 \\ 0 & \partial^2_m & 0 \\ 0 & 0 & \partial^2_{m+1} \end{pmatrix}. \tag{5.11}$$

The solution of the equations for the m-th Fourier mode with $m \neq 0$ proceeds as follows: first, the transformation $\boldsymbol{\Theta}$ is applied to the Fourier coefficient $\boldsymbol{f}_m$ of the source term $\boldsymbol{f}$ of the Poisson equation, then solve the three uncoupled elliptic 2D equations and finally perform the inverse transformation to the spherical components, as summarised as follows

$$\begin{pmatrix} f^1_{m-1} \\ f^2_m \\ f^3_{m+1} \end{pmatrix} = \boldsymbol{\Theta} \begin{pmatrix} f^r_m \\ f^\theta_m \\ f^\phi_{-m} \end{pmatrix} \qquad \begin{aligned} -\partial^2_{m-1}u^1_{m-1} &= f^1_{m-1}(r,\theta); \\ -\partial^2_m u^2_m &= f^2_m(r,\theta); \\ -\partial^2_{m+1}u^3_{m+1} &= f^3_{m+1}(r,\theta); \end{aligned} \qquad \begin{pmatrix} u^r_m \\ u^\theta_m \\ u^\phi_{-m} \end{pmatrix} = \boldsymbol{\Theta}^T \begin{pmatrix} u^1_{m-1} \\ u^2_m \\ u^3_{m+1} \end{pmatrix}. \tag{5.12}$$

The problem for the first Fourier mode $m = 0$ is simpler, since the corresponding matrix operator in the Fourier space is

$$\boldsymbol{\partial}^2_0 = \begin{pmatrix} \partial^2_0 - \frac{2}{r^2} & -\frac{2}{r^2\sin\theta}\frac{\partial}{\partial\theta}(\sin\theta\ldots) & 0 \\ \frac{2}{r^2}\frac{\partial}{\partial\theta} & \partial^2_1 & 0 \\ 0 & 0 & \partial^2_1 \end{pmatrix}. \tag{5.13}$$

Thus, the similarity transformation performing the diagonalisation is easily found to be

$$\boldsymbol{\Theta}_0\boldsymbol{\partial}^2_0\boldsymbol{\Theta}_0 = \begin{pmatrix} \partial^2_1 & 0 & 0 \\ 0 & \partial^2_0 & 0 \\ 0 & 0 & \partial^2_1 \end{pmatrix}. \tag{5.14}$$

The solution procedure for the first mode $m = 0$ amounts therefore to transforming the source term $\boldsymbol{f}_0$ by means of matrix $\boldsymbol{\Theta}_0$, followed by the solution of the three uncoupled equations and by the inverse transformation, as follows

$$\begin{pmatrix} f^1_{-1} \\ f^2_0 \\ f^3_1 \end{pmatrix} = \boldsymbol{\Theta}_0 \begin{pmatrix} f^r_0 \\ f^\theta_0 \\ f^\phi_0 \end{pmatrix}, \qquad \begin{aligned} -\partial^2_1 u^1_{-1} &= f^1_{-1}(r,\theta); \\ -\partial^2_0 u^2_0 &= f^2_0(r,\theta); \\ -\partial^2_1 u^3_1 &= f^3_1(r,\theta); \end{aligned} \qquad \begin{pmatrix} u^r_0 \\ u^\theta_0 \\ u^\phi_0 \end{pmatrix} = \boldsymbol{\Theta}_0 \begin{pmatrix} u^1_{-1} \\ u^2_0 \\ u^3_1 \end{pmatrix}. \tag{5.15}$$

The truncated version of Fourier expansion (5.2) is given by taking the upper summation extreme equal to $M_t - 1$ so that the term $\boldsymbol{u}_{M_t}$ of the vector expansion is absent.

After the uncoupling, the new scalar unknowns are expanded in the associated Legendre functions, as done for the scalar problem.For the general modes with $m \neq 0$ the expansion is

$$\begin{aligned} u^1_{m-1}(r,\theta) &= \sum_{\ell=|m-1|}^{M_t} u_\ell^{m-1;1}(r)\widehat{P}_\ell^{|m-1|}(\cos\theta), \\ u^2_{m}(r,\theta) &= \sum_{\ell=|m|}^{M_t} u_\ell^{m;2}(r)\widehat{P}_\ell^{|m|}(\cos\theta), \\ u^3_{m+1}(r,\theta) &= \sum_{\ell=|m+1|}^{M_t} u_\ell^{m+1;3}(r)\widehat{P}_\ell^{|m+1|}(\cos\theta), \end{aligned} \tag{5.16}$$

and the same expressions with $m = 0$ apply also to the first special vector mode $m = 0$.

5.3. Numerical results

To test the spectral solvers for the vector Dirichlet problem in spherical domains, the exact solution must be constructed so as to give an infinitely differentiable vector field also on the z axis, including the origin which is the sphere center. This requires to define the vector field in terms of its Cartesian components, in addition to be a function of the Cartesian coordinates. In our tests the exact solution is chosen to be the vector field defined as follows:

$$\begin{aligned} u_x &= e^{p_1(x-x_1)^2+q_1(y-y_1)^2+z-z_1} \\ u_y &= e^{p_2(x-x_2)^2+q_2(y-y_2)^2+z-z_2} \\ u_z &= e^{p_3(x-x_3)^2+q_3(y-y_3)^2+z-z_3} \end{aligned}$$

with all the parameters given by

$$\begin{aligned} &p_1 = 0.5, \quad q_1 = 1.2, \quad x_1 = 0.1, \quad y_1 = 0.2, \quad z_1 = 0.3; \\ &p_2 = 0.7, \quad q_2 = 1.4, \quad x_2 = 0.2, \quad y_2 = 0.3, \quad z_2 = 0.4; \\ &p_3 = 0.9, \quad q_3 = 1.6, \quad x_3 = 0.3, \quad y_3 = 0.4, \quad z_3 = 0.5. \end{aligned}$$

The L^2_w norm of a vector function is defined, as it is standard, by

$$\|\boldsymbol{u}\|^2_{L^2_w} = \|u^r\|^2_{L^2_w} + \|u^\theta\|^2_{L^2_w} + \|u^\phi\|^2_{L^2_w}.$$

5.3.1. Spherical gap

The errors of the spectral solutions in the spherical gap $0.5 \leqslant r \leqslant 1.5$ are reported in Table 12 and demonstrate the spectral convergence of the uncoupled vector solver.

Table 12
Vector Dirichlet problem for Helmholtz operator with $\gamma = 1.5$ in the spherical gap $0.5 \leqslant r \leqslant 1.5$

$N = M_t$	L^∞ error	L^2_w error
15	1.7×10^{-3}	1.1×10^{-3}
20	7.1×10^{-6}	4.3×10^{-6}
25	1.5×10^{-8}	8.7×10^{-9}
30	1.4×10^{-11}	9.6×10^{-12}
35	1.6×10^{-12}	6.2×10^{-13}
40	3.3×10^{-12}	9.0×10^{-13}
45	4.1×10^{-12}	1.1×10^{-12}
50	2.3×10^{-12}	7.0×10^{-13}

Exact solution: see the text.

Table 13
Vector Dirichlet problem for Helmholtz operator with $\gamma = 1.5$ inside the unit sphere $\rho \leqslant 1$

M_t	L^∞ error	L^2_w error
15	6.1×10^{-2}	2.8×10^{-2}
20	4.8×10^{-4}	1.8×10^{-4}
30	2.8×10^{-9}	1.0×10^{-9}
40	7.2×10^{-12}	4.4×10^{-12}
50	1.3×10^{-11}	1.3×10^{-11}

Exact solution: see the text.

5.3.2. Sphere

The uncoupled algorithm can be used also in the case of a spherical domain. In this case the lifted matrix for the scalar problems of the different spectral components is $\mathsf{A}_{\boxed{\ell}} = \mathsf{D}_{\boxed{\ell}} + \gamma \mathsf{M}_{\boxed{\ell}}$, so that the uncoupled scalar equations for the vector unknown will be

$$\begin{aligned} \mathsf{A}_{\boxed{\ell}} \mathsf{u}^{m-1;1}_{\boxed{\ell}} &= \mathsf{g}^{m-1;1}_{\boxed{\ell}} - A^s_{\boxed{\ell}} a^{m-1;1}_{\boxed{\ell}}, \\ \mathsf{A}_{\boxed{\ell}} \mathsf{u}^{m;2}_{\boxed{\ell}} &= \mathsf{g}^{m;2}_{\boxed{\ell}} - A^s_{\boxed{\ell}} a^{m;2}_{\boxed{\ell}}, \\ \mathsf{A}_{\boxed{\ell}} \mathsf{u}^{m+1;3}_{\boxed{\ell}} &= \mathsf{g}^{m+1;3}_{\boxed{\ell}} - A^s_{\boxed{\ell}} a^{m+1;3}_{\boxed{\ell}}. \end{aligned}$$

The errors of the spectral solutions with $\gamma = 1.5$ of the vector Dirichlet problem in the unit sphere $\rho \leqslant 1$ with $p_i = i$ and $q_i = i + 1$, for $i = 1,2,3$, are reported in Table 13. These results demonstrate the spectral convergence of a vector solution arbitrarily defined up to the center of the sphere.

6. Conclusion

In this paper a suite of Galerkin spectral solvers for scalar and vector Helmholtz equations in spherical coordinates has been presented. The ultimate aim of our effort is to build a full set of spectral algorithms suitable for the numerical solution of the incompressible Navier–Stokes equations in spherical domains by means of fractional step projection method, as done for rectangular domains in [2]. This method requires in fact to solve at each time step a Poisson equation supplemented by Neumann boundary condition for the pressure and a vector Helmholtz equation supplemented typically by Dirichlet conditions on the spherical boundaries for the velocity. Three bases have been presented, depending on the kind of boundary conditions to be satisfied and on whether the computational domain is a sphere or a spherical gap. For the Neumann scalar problem in the spherical gap, a simple rescaling of Legendre polynomials has been adopted as the basis function, while for the Dirichlet problem one of the bases proposed in [15] has been employed. In the case of the full sphere including the center, a new Jacobi one-sided basis has been adopted for both Neumann and Dirichlet problems.

The basic idea underlying the new spectral solvers for the spherical domain is that, exactly as fewer associated Legendre functions are needed for the approximate representation of latitudinal variations of higher Fourier modes, also fewer Jacobi polynomials are needed for the resolution of the radial structure of higher latitudinal modes. This simple principle leads to an optimal truncation scheme for the finite spectral approximation of functions behaving analytically inside a sphere, in the sense that the number of required degrees of freedom is minimal. From the algorithmic viewpoint, a peculiarity of the proposed elliptic solvers is that linear systems of decreasing order are involved in the solution of the radial spectral equations associated with higher latitudinal, and therefore also longitudinal, modes. As a final result, the Jacobi basis employed here to resolve radial variations of the solution does not face any difficulty with the sphere centre much in the same manner the spherical harmonic functions suffer no problem on the polar axis.

In all Dirichlet problems considered in this paper, nonhomogeneous boundary values are accounted for by means of a lifting implemented at the discrete level. As far as the solution of the vector Dirichlet problem is concerned, an original uncoupled solution algorithm has been implemented which is based on the solution of scalar and real equations only and which is effective to provide spectrally convergent values of the vector field

up to the polar axis and the sphere centre. Remarkably enough, for the simulation of unsteady incompressible flows inside a sphere, the proposed spectral basis, thanks to its ability to satisfy all the regularity conditions at the centre, is devoid of any over resolution there and is expected to free the time integration from severe time step restrictions.

Acknowledgments

The authors wish to thank gratefully Paolo Luchini and Lorenzo Valdettaro for their useful suggestions which helped to enhance the content of the present paper. The authors are also grateful to two reviewers for their comments that simplified and enriched the presentation.

References

[1] E. Anderson et al., LAPACK, third ed., SIAM, Philadelphia, 1999.
[2] F. Auteri, N. Parolini, A mixed-basis spectral projection method, J. Comput. Phys. 175 (2002) 1–23.
[3] F. Auteri, L. Quartapelle, Algorithms for the spectral solution of 3D elliptic problems in spherical regions, Scientific Report, DIA SR-06-06.
[4] S. Bonazzola, J.-A. Mark, Three-dimensional gas dynamics in a sphere, J. Comput. Phys. 87 (1990) 201–230.
[5] J.P. Boyd, Chebyshev and Fourier Spectral Methods, Dover, New York, 2001.
[6] M.-C. Lai, W.-W. Lin, W. Wang, A fast spectral/difference method without pole conditions for Poisson-type equations in cylindrical and spherical geometries, IMA J. Num. Anal. 22 (2002) 537–548.
[7] G.A. Glatzmaier, Numerical simulations of stellar convective dynamos, J. Comp. Phys. 55 (1984) 461–484.
[8] R. Hollerbach, A spectral solution of magneto-convection equations in a spherical geometry, Int. J. Num. Meth. Fluids 15 (2000) 773–797.
[9] A. Kageyama, S. Kida, A spectral methods in spherical coordinates with coordinate singularity at the origin, NIFS (National Institute for Fusion Science, Report 636, 2000, http://www.nifs.ac.jp/report/NIFS-636.pdf.
[10] B. Machenhauer, R. Daley, A baroclinic primitive equation model with a spectral representation in three dimensions, Report No. 4, Institut for Teoretisk Meteorologi, Kobenhavns Universitet, Denmark, 1972.
[11] P.A. Marcus, L. Tuckermann, Simulation of flow between concentric rotating spheres. Part 1 Steady states, J. Fluid Mech. 185 (1987) 1–65.
[12] S.A. Orszag, Fourier series on spheres, Monthly Weather Rev. 102 (1974) 56–75.
[13] L. Quartapelle, Numerical Solution of the Incompressible Navier–Stokes Equations, Birkhäuser, Basel, 1993.
[14] Jie Shen, Efficient spectral–Galerkin method. I. Direct solvers of second- and fourth-order equations using Legendre polynomials, SIAM J. Sci. Comput. 15 (1994) 1489–1505.
[15] Jie Shen, Efficient spectral–Galerkin methods. IV. Spherical geometries, SIAM J. Sci.Comput. 20 (1999) 1438–1455.
[16] P.N. Swarztrauber, The approximation of vector functions and their derivatives on the sphere, SIAM J. Numer. Anal. 16 (1981) 191–210.
[17] P.N. Swarztrauber, The vector harmonic transform method for solving partial differential equations in spherical geometry, Monthly Weather Rev. 124 (1993) 3415–3437.